IAU: Multi-scale (time and mass) dynamics of space object Symposium
Proceedings of the IAU Symposium No. 364, 2021 No. ,
A. Celletti, C. Beaugé, C. Galeş, A. Lemaître, eds.
doi:

Multiple bifurcations around 433 Eros with Harmonic Balance Method

Leclère Nicolas[1], Kerschen Gaëtan[1], and Dell'Elce Lamberto[2]

[1]Space Structures and Systems Laboratory, Department of Aerospace and Mechanical Engineering, Université de Liège, Belgique
[2]Inria & Université Côte Azur, McTAO team, Sophia Antipolis, France.

Abstract. The objective of this paper is to carry out periodic orbital propagation and bifurcations detection around asteroid 433 Eros. Specifically, we propose to exploit a frequency-domain method, the harmonic balance method, as an efficient alternative to the usual time integration. The stability and bifurcations of the periodic orbits are also assessed thanks to the Floquet exponents. Numerous periodic orbits are found with various periods and shapes. Different bifurcations, including period doubling, tangent, real saddle and Neimark-Sacker bifurcations, are encountered during the continuation process. Resonance phenomena are highlighted as well.

Keywords. Harmonic balance, asteroid, Eros, bifurcations, resonance

1. Introduction

Interest in asteroids and small celestial bodies significantly increased in the last two decades, and, consequently, the number of space exploration missions increased as well. Concerning the orbital propagation around asteroids and the study of the bifurcations of their periodic orbits, one of the methods considered is the grid searching method proposed by Yu & Baoyin (2012). It was applied to compute families of orbits around 216 Kleopatra Yu & Baoyin (2012); a summary of all the classifications of bifurcations was proposed by Jiang (2015). This paper focuses on orbital dynamics about 433 Eros, which was subject of recent studies Ni (2016), Scheeres (2000). The rotation period of 433 Eros is of 5.270 hours and the density is equal to 2.673 g/cm^3. The focus of this study is made on the method applied for the computation of periodic orbits and the detection of the bifurcation. The harmonic balance method is applied to the equation of motion offering a new and unique approach to compute periodic solutions. The paper is organized as follows. First, details on the polyhedron method for the gravitational modeling of the asteroid are briefly recalled. Then, the harmonic balance method, used for orbital propagation, is introduced. Finally, the obtained results are exposed.

2. Polyhedron method

The polyhedron method introduced by Werner (1994) is extensively used to model the gravitational field of irregular celestial bodies like asteroids. The method is based on the construction of a surface mesh with the assumption that the density of the body is constant. Some meshes were generated from radar observations, others are the direct result of on-site observations during specific missions, e.g., NASA mission *Osiris-REX* on 101955 Bennu, ESA mission *Rosetta* on 67P Churyumov–Gerasimenko and JAXA mission *Hayabusa* on 25143 Itokawa Tsuchiyama (2011). The polyhedron model of 433 Eros is the result of NASA mission *NEAR Shoemaker* Veverka (2001). Figure 1 shows the mesh of 433 Eros, consisting of 856 vertices and 1708 faces.

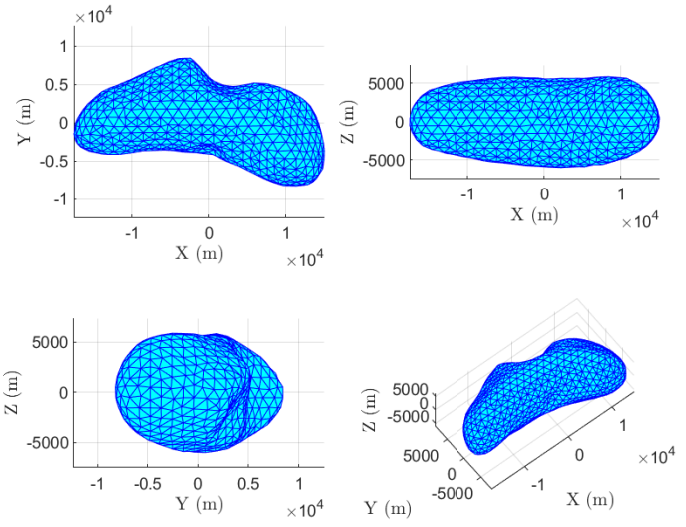

Figure 1: Polyhedron model of 433 Eros

The main advantage of the polyhedron method is the simple computation of the gravitational potential of the celestial body, U, namely

$$U = \frac{1}{2} G\rho \sum_{edges} (\mathbf{r}_e \cdot \mathbf{E}_e \cdot \mathbf{r}_e) \cdot L_e - \frac{1}{2} G\rho \sum_{faces} \left(\mathbf{r}_f \cdot \mathbf{F}_f \cdot \mathbf{r}_f\right) \cdot \omega_f \tag{1}$$

where ρ is the bulk density of the body, G is the gravitational constant, the two vectors $\mathbf{r}_e$ and $\mathbf{r}_f$ are body-fixed vectors from the particle to the edge e and the face f, respectively. Matrices $\mathbf{E}_e$ and $\mathbf{F}_f$ gather the geometric parameters of the edges e and faces f. $\mathbf{L}_e$ denotes the integration factor of the particle position and the edge e whereas ω_f corresponds to the solid angle of the face f relative to the particle.

The gradient of the gravitational potential is then easily obtained

$$\nabla U = -G\rho \sum_{edges} (\mathbf{E}_e \cdot \mathbf{r}_e) \cdot L_e + G\rho \sum_{faces} \left(\mathbf{F}_f \cdot \mathbf{r}_f\right) \cdot \omega_f \tag{2}$$

This expression of the gravitational potential yields the equation of motion in the co-rotating frame

$$\ddot{\mathbf{x}} + 2\omega_\mathbf{a} \times \dot{\mathbf{x}} + \omega_\mathbf{a} \times (\omega_\mathbf{a} \times \mathbf{x}) + \nabla U(\mathbf{x}) = 0 \tag{3}$$

The body-fixed vector that links the asteroid body's center of mass to the particle is denoted $\mathbf{x}$, ω_a represents the angular velocity of the asteroid. The harmonic balance method is used to compute solutions to this equation.

3. Harmonic Balance

The harmonic balance method aims at approximating periodic solutions of the equations of motion, $x(t)$, by means of a Fourier series truncated to the N-th harmonic, namely

$$x(t) = \frac{c_0^x}{\sqrt{2}} + \sum_{k=1}^{N_H} \left(s_k \sin(k\omega t) + c_k \cos(k\omega t)\right) \tag{4}$$

A similar decomposition is carried out for the nonlinear force ∇U. Vectors s_k and c_k are the Fourier coefficients associated to the sine and cosine, respectively. ω corresponds to the frequency of the periodic orbit (which is not correlated to the angular velocity of the asteroid, ω_a). The Fourier coefficients are gathered in a new vector $\mathbf{z}$ for the displacement and $\mathbf{b}$ for the nonlinear force of dimension $(2N_H + 1)\, n \times 1$, with n the degrees of freedom of the studied system. Equation 3 can eventually be rewritten as

$$\mathbf{h}(\mathbf{z}, \omega) = \mathbf{A}(\omega)\mathbf{z} - \mathbf{b}(\mathbf{z}) = \mathbf{0} \tag{5}$$

where matrix $\mathbf{A}$ describes the linear dynamics. A predictor-corrector algorithm is used to solve Equation 5, as proposed in Detroux (2014). This approach presents numerous advantages over the classical time integration method. Working in the frequency domain provides a fast and efficient alternative from time domain methods to solve the equation of motion. The predictor-corrector algorithm is a great tool to compute orbit families.

The stability of orbits, as well as the detection of bifurcations, can be determined through the Floquet multipliers which are the eigenvalues of the monodromy matrix Peletan (2013). In the frequency domain, an alternative method known as Hill's method exists. It consists in introducing the periodic solution $\mathbf{x}^*(t)$ perturbed with another periodic solution $\mathbf{s}(t)$ modulated by an exponential decay into the equation of motion, Eq. 3.

$$\mathbf{p}(t) = \mathbf{x}^*(t) + e^{\lambda t}\mathbf{s}(t) \tag{6}$$

which eventually leads to the simple quadratic eigenvalue problem

$$\left(\Delta_2 \lambda^2 + \Delta_1 \lambda + \mathbf{h_z}\right) \mathbf{u} = \mathbf{0} \tag{7}$$

that provides the Floquet mutlipliers, λ. If two multipliers cross at +1 on the unit circle the bifurcation is a tangent bifurcation. If the crossing happens at -1, it is a period doubling bifurcation. We refer to a real saddle if two multipliers leave the real axis as complex conjugates; if they leave the unit circle as complex conjugates, there is the presence of a Neimark Sacker bifurcation. A graphical depiction summarizes the different cases in Figure 2. Δ_1 and Δ_2 also describe the linear dynamic. $\mathbf{h_z}$ is the derivative of equation 5 with respect to $\mathbf{z}$. The vector $\mathbf{u}$ is the equivalent of $\mathbf{z}$ but for the Fourier coefficients of $\mathbf{s}$.

4. Results

We consider the continuation process between the periodic ratios, $\frac{\omega}{\omega_a}$ starting from approximately 2 up to 3. The results of the continuation are displayed in Figure 3, each point in this plot correspond to a unique periodic orbit. We refer to each group of orbits separated by bifurcations as families. They are gathered in Table 1.

Most bifurcations are located around resonant periods, associated to the nominal period ratio 2:1 and 3:1, where Jacobi's constant changes abruptly, whereas it remains roughly

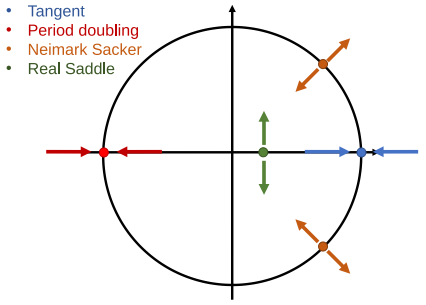

Figure 2: Bifurcations classified thanks to Floquet multipliers

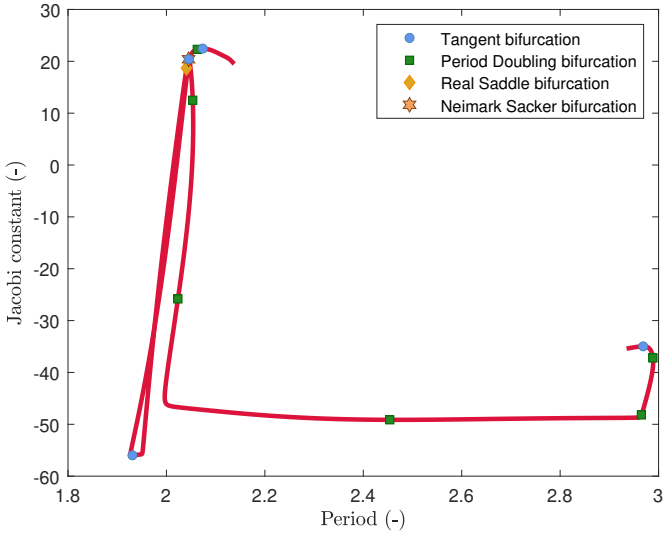

Figure 3: Continuation process between the periodic ratio of 2 and 3 with regard to the Jacobian constant

constant in between. There is just a period doubling bifurcation between the two resonances around the ratio 2.5:1. It is in fact a quasi-period doubling bifurcation, meaning that the Floquet multipliers simply cross the value -1 on the unit circle and remain on it afterwards Kang (2018).

The stable region identified during the continuation process, corresponding to family 6, is displayed in black in Figure 4. The stability appears between a Neimark Sacker bifurcation and a tangent bifurcation.

Figure 5 displays representative orbits for each family. The unfolding of the few first families can clearly be observed. After family 4, the shape of the orbits is rotated by 90 degrees compared to those in family 3. Starting from family 8, the orbits begin to flatten to the point

Family n°	Period ratio	Jacobian constant	Bifurcation	Stability
1	]2.138;2.074]	]19.496;22.451]	Tangent	U
2	]2.074;2.063]	]22.451;22.324]	Period Doubling	U
3	]2.063;1.931]	]22.324;-55.984]	Tangent	U
4	]1.931;2.041]	]-55.984;18.689]	Real Saddle	U
5	]2.041;2.045]	]18.689;20.395]	Neimark Sacker	U
6	]2.045;2.0455]	]20.395;20.411]	Tangent	S
7	]2.0455;2.053]	]20.411;12.504]	Period Doubling	U
8	]2.053;2.023]	]12.504;-25.824]	Period Doubling	U
9	]2.023;2.454]	]-25.824;-49.136]	Period Doubling	U
10	]2.454;2.965]	]-49.136;-48.199]	Period Doubling	U
11	]2.965;2.989]	]-48.199;-37.213]	Period Doubling	U
12	]2.989;2.969]	]-37.213;-34.969]	Period Doubling	U
13	]2.969;2.935]	]-34.969;-35.409]	Tangent	U

Table 1. : Bifurcations, stability and period ratio of the orbit families

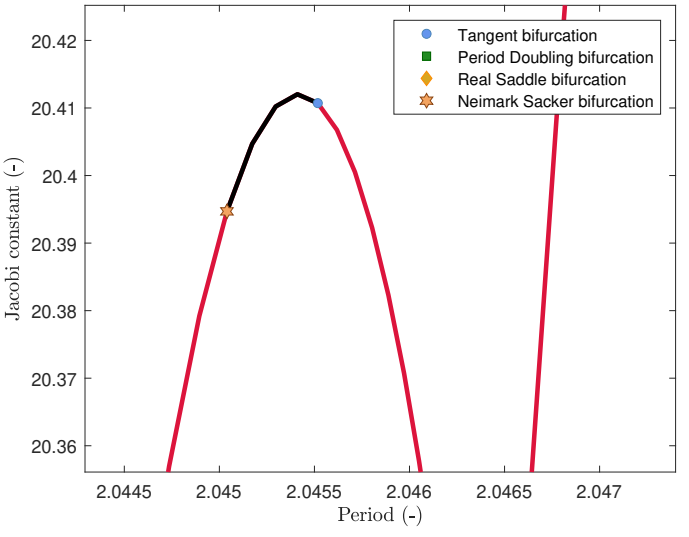

Figure 4: Focus on the stable orbits during the continuation.

that family 10 has orbits with almost zero inclination. Families 11, 12 and 13 evolve into more complex orbits.

5. Conclusion

In this paper, a new approach for the computation of periodic orbits around asteroids is proposed. The harmonic balance method is introduced, and its application to the detection of bifurcation and search for periodic orbits around the asteroid 433 Eros is presented. Twelve bifurcations of different types are encountered mainly around the resonances 2:1 and 3:1. The stability of the orbits is also studied and only one family of orbits is found to be stable.

References

Detroux, T., Renson, L., Kerschen, G. . 2014 The harmonic balance method for advanced analysis and design of nonlinear mechanical systems. Conf. Proc. Soc. Exp. Mech. S. 2, 19-34

Jiang, Y., Yu, Y., Baoyin, H. 2015 Topological classifications and bifurcations of periodic orbits in the potential field of highly irregular-shaped celestial bodies. Nonlinear Dyn. 81(1–2), 119–140

Kang, H., Jiang,Y., Li, H. 2018 Pseudo Bifurcations and Variety of Periodic Ratio for Periodic Orbit Families Close to Asteroid (22) Kalliope. Planetary and Space Sci.

Ni, Y., Jiang, Y., Baoyin, H. 2016 Multiple bifurcations in the periodic orbit around Eros. Astriohys Space Sci. 361:170

Peletan, L., Baguet, S., Torkhani, M., Jacquet-Richardet G. 2013 A comparison of stability computational methods for periodic solution of nonlinear problems with application to rotordynamics. Nonlinear Dynamics. 72(3), 671:682

Scheeres, D.J., Williams,B.G., Miller, J.K. 2000 Evaluation of the Dynamic Environment of an Asteroid: Applications to 433 Eros. Journal of Guidance, Control and Dynamics Vol. 23 No. 3

Tsuchiyama, A., Uesugi,M., Matsushima, T., et al. 2011 Three-dimensional structure of Hayabusa samples: origin and evolution of Itokawa regolith. Science 333(6046), 1125–1128

Veverka, J., Farquhar, B., Robinson, M., et al. 2001 The landing of the NEAR-Shoemaker spacecraft on asteroid 433 Eros. Nature 413(6854), 390–393

Werner, G.A. 1994 The gravitational potential of a homogeneous polyhedron or don't cut corners. Celest. Mech. Dyn. Astron. 59(3), 253–278

Yu, Y., Baoyin, H., Jiang, Y. 2015 Constructing the natural families of periodic orbits near irregular bodies. Mon. Not. R. Astron. Soc. 453(1), 3269–3277

Yu, Y., Baoyin, H. 2012 Generating families of 3D periodic orbits about asteroids. Mon. Not. R. Astron. Soc. 427(1), 872–881

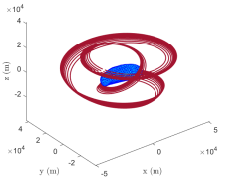

(a) Family n°1

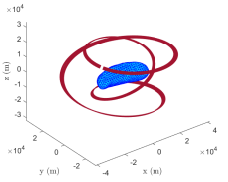

(b) Family n°2

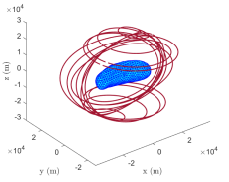

(c) Family n°3

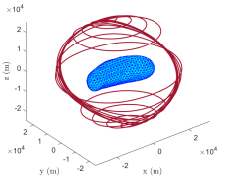

(d) Family n°4

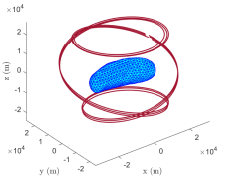

(e) Family n°5

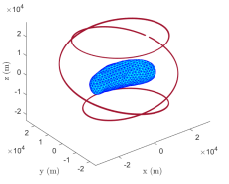

(f) Family n°6

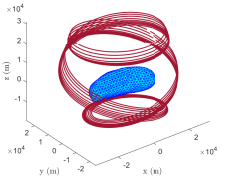

(g) Family n°7

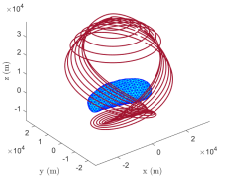

(h) Family n°8

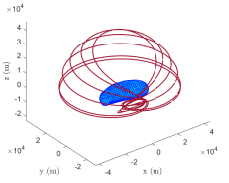

(i) Family n°9

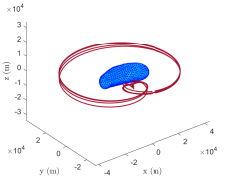

(j) Family n°10

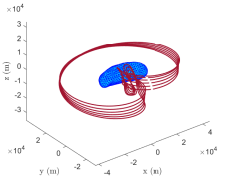

(k) Family n°11

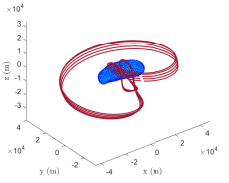

(l) Family n°12

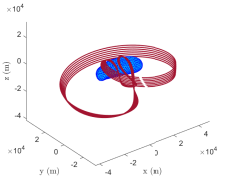

(m) Family n°13

Figure 5: Families of periodic orbits around 433 Eros